Journal of Thermal Analysis, Vol. 46 (1996) 1201-1213

STUDIES ON THE DEHYDRATION AND DECOMPOSITION OF CALCIUM AND DICALCIUM MAGNESIUM ACONITATE HYDRATES

W. O. S. Doherty, O. L. Crees**, C. Cuff* and E. Senogles**

*James Cook University of North Queensland, Townsville, Australia
**Sugar Research Institute, Mackay, Australia

(Received March 1, 1995)

Abstract

The thermal decomposition of calcium and dicalcium magnesium aconitate hydrates were studied by TG/DTG, DTA, EGA, SEM and other physico-chemical techniques. The decomposition proceeds in four stages: dehydration; oxidation of the carboxylic acid portion of the salt; complete fragmentation of the hydrocarbon portion; and finally, decarboxylation of the metal carbonate to the oxide. The crystal morphologies of the hydrate and anhydrous salts of each compound are very similar. Tricalcium aconitate consists of well-developed twinned crystals and stellate clusters intergrown with flat platy crystals. On the other hand, dicalcium magnesium aconitate crystals are monoclinic with well-developed pinacoidal faces.

The activation energy, E_d (43±2 kJ mol^{-1} water), calculated from Borchardt and Daniels' method, for the dehydration process of calcium aconitate trihydrate is of the same order of magnitude as some simple metal salt hydrates. The rate constant, k_d increased from 0.04/min at 238°C to greater than 0.86/min at 295°C. It is concluded that the dehydration process is due to cation bound water.

Keywords: calcium aconitate, DTA, EGA, kinetics, SEM, TG/DTG, thermal decomposition

Introduction

Derivatives of aconitic acid have many industrial applications. For example, they are used as plasticisers, surface-active agents, antioxidants and flavouring agents [1, 2]. Itaconic acid, prepared by decarboxylation of aconitic acid, is used in the synthesis of polymeric materials such as alkyd resins [2]. Aconitic acid is prepared from sugar cane syrups and molasses (where it constitutes about two-third of the organic acid portion) through the addition of calcium and magnesium chlorides and the treatment of the precipitate with a cation exchange resin. It is precipitated as dicalcium magnesium aconitate hexahydrate, $Ca_2Mg(C_6H_3O_6)_2 \cdot 6H_2O$, and to a lesser extent, calcium aconitate trihydrate, $Ca_3(C_6H_3O_6)_2 \cdot 3H_2O$, and other hydrate phases. These compounds are also pre-

0368–4466/96/ $ 5.00

John Wiley & Sons, Limited
Chichester

sent in scales formed in evaporators of sugar mills, which cause the lowering of heat transfer coefficients and consequent reduction in the crushing rates of the mills [1, 3]. Because of this, mills have to shut down regularly so that the scale deposits can be removed by chemical and/or mechanical means and operation efficiency restored.

In view of the technological significance of the aconitates, there has been renewed interest in their preparation, dehydration, decomposition, crystallographic forms, morphologies, and crystallisation inhibition from supersaturated solutions by polyelectrolytes [3, 4]. Hitherto there has been no study reported on the dehydration and decomposition of these hydrates. This paper presents such studies using thermogravimetry (TG) and derivative thermogravimetry (DTG), evolved gas analysis (EGA), differential thermal analysis (DTA) and a variety of physico-chemical techniques. The DTA curve for the dehydration of $Ca_3(C_6H_3O_6)_2 \cdot 3H_2O$ was further analysed to give the kinetics of the process. This process was evaluated by Borchardt and Daniels' method [5]. some scanning electron microscopy (SEM) studies on the hydrate and dehydrated salts were also carried out.

Experimental

Materials and solutions

Trans-aconitic acid was supplied by Aldrich Inc. Calcium chloride and potassium hydroxide were British Drug House A.R. materials. Calcium carbonate and magnesium oxide were G.P.R. materials also supplied by British Drug House Ltd.

Stock solutions were prepared in cold carbon dioxide-free distilled water and were standardised by recommended procedures.

Preparation of hydrates

Tricalcium aconitate trihydrate, $Ca_3(C_6H_3O_6)_2 \cdot 3H_2O$

This salt was prepared by a method first described by Ambler *et al.* [7]. Freshly prepared 0.2 *M* potassium aconitate (obtained by neutralising aconitic acid with potassium hydroxide) was rapidly added to a slight excess of 0.3 *M* calcium chloride and the mixture, without agitation, maintained at 85°C in a water bath. Prior to mixing, the *pH* of each solution was adjusted to 6.0 and kept at 85°C. Crystallisation was induced by rubbing the sides of the flask with a glass rod. The precipitate formed was left to digest in the hot solution for 15 min before filtering it and washing repeatedly with hot distilled water. Residual water was removed by drying at ambient temperature under vacuum to constant weight.

Dicalcium magnesium aconitate hexahydrate, $Ca_2Mg(C_6H_3O_6)_2 \cdot 6H_2O$

This salt was also prepared by the method of Ambler *et al.* [6]. 0.2 *M* aconitic acid was two-third neutralised with calcium carbonate and the resulting solution brought to $pH=6.5$ with magnesium oxide and filtered. The filtrate was heated in a steam bath for three hours at 95°C. Crystallisation was induced with a glass rod and the precipitate at the end of the three hours washed and dried as described previously.

Chemical compositions

Precipitate compositions were determined by atomic absorption spectrophotometry (AAS), elemental analysis, chemical analysis, thermal analysers (TG/DTG and DTA) and SEM. Crystal sizes and shapes were examined with a Philips XL 20 series SEM operating at a gun voltage of 20 kV.

Dehydration and decomposition of the hydrates

TG/DTG and DTA

These measurements were carried out in the Advanced Materials Laboratory, Australian Nuclear Science and Technology Organisation Sydney, Australia. Samples (14–17 mg) were heated in a Setaram TAG 24 simultaneous DTA/TG analyser at 10°C min^{-1} from room temperature up to 1000°C in a flowing air atmosphere. The reference sample was calcined alumina ground to the same particle size as the sample. The instrument was calibrated by measurements of the temperatures and enthalpies of fusion of known weights of tin, indium and gold.

EGA

These measurements were carried out at the Thermal Characterisation Laboratory, Curtin University of Technology, Perth, Australia. Approximately 10 mg of sample was heated at 10°C min^{-1} in an oxidising atmosphere (20% v/v oxygen in nitrogen). The gases evolved in the thermal treatment were transferred from the thermal analyser to a Bruker IFS 55 infrared (IR) spectrometer via a heated line held constant at 220°C. The spectrometer monitored from 4000–650 cm^{-1} and the specific regions 2400–2250 cm^{-1}, 2210–2155 cm^{-1} and 2000–1300 cm^{-1} for CO_2, CO and H_2O respectively.

Kinetics

Despite comments that the approach of Borchardt and Daniels is not applicable to solid-state reactions [7], a number of workers [8–12] have applied it to

various dehydration, decomposition and crystallisation processes. In this study, the $Ca_3(C_6H_3O_6)_2{\cdot}3H_2O$ dehydration curve was analysed using this method. According to this treatment, the rate constant for dehydration at any temperature (k_d) is given by,

$$k_d = \frac{\Delta T}{A - a} \tag{1}$$

where ΔT is the temperature difference between the reference junction and the sample junction of the thermocouples; A is the total area under the curve and a the area at any time t.

Assuming that DTA traces approximate to triangles,

$$a = \frac{t \times \Delta T}{2} \tag{2}$$

and therefore

$$k_d = \frac{2a}{t(A - a)} \tag{3}$$

If α_{dt} is the extent of the reaction after any time,

$$\alpha_{dt} = \frac{a}{A} \tag{4}$$

and

$$k_d = \frac{2\alpha_{dt}}{t(1 - \alpha_{dt})} \tag{5}$$

In addition an estimation of initial reaction rate at one temperature was obtained using the modified approach of Borchardt [13] reported to be applicable to solid-state reactions.

In order to complement the thermal analyses, elemental analysis, AAS, XRD and SEM were used at various stages of the dehydration and decomposition processes. The XRD studies were carried out using a Rigaku camera and a X-ray generator with CuK_α radiation of wavelength 1.5148 Å.

Results and discussion

Precipitate compositions

The physico-chemical analyses indicated that the tricalcium aconitate and dicalcium magnesium aconitate hydrates prepared under these conditions were $Ca_3(C_6H_3O_6)_2{\cdot}3H_2O$ and $Ca_2Mg(C_6H_3O_6)_2{\cdot}6H_2O$ respectively; they were devoid of other hydrate phases, calcite and magnesium oxide.

Thermal analyses

TG/DTG and DTA curves for the dehydration and decomposition of $Ca_3(C_6H_3O_6)_2 \cdot 3H_2O$ are presented in Fig. 1. The TG/DTG curves indicate three distinct mass losses. The first mass loss, at temperatures from ca 179–355°C, corresponds to the loss of the three water molecules (12%), and the second (25%) and third (30%) mass losses occurring from 428–507°C and 649–776°C respectively, likely correspond to the decomposition of the anhydrous tricalcium aconitate.

The DTA curve in Fig. 1 shows two endothermic reactions from 179–355°C and 649–781°C. There is also a predominant exothermic reaction from 436–529°C; this exotherm has a shoulder at 495°C. The first peak with a minimum of 282°C corresponds to the loss of the hydrate water molecules; the next with a peak maximum at 477°C is more likely the result of the oxidation of vola-

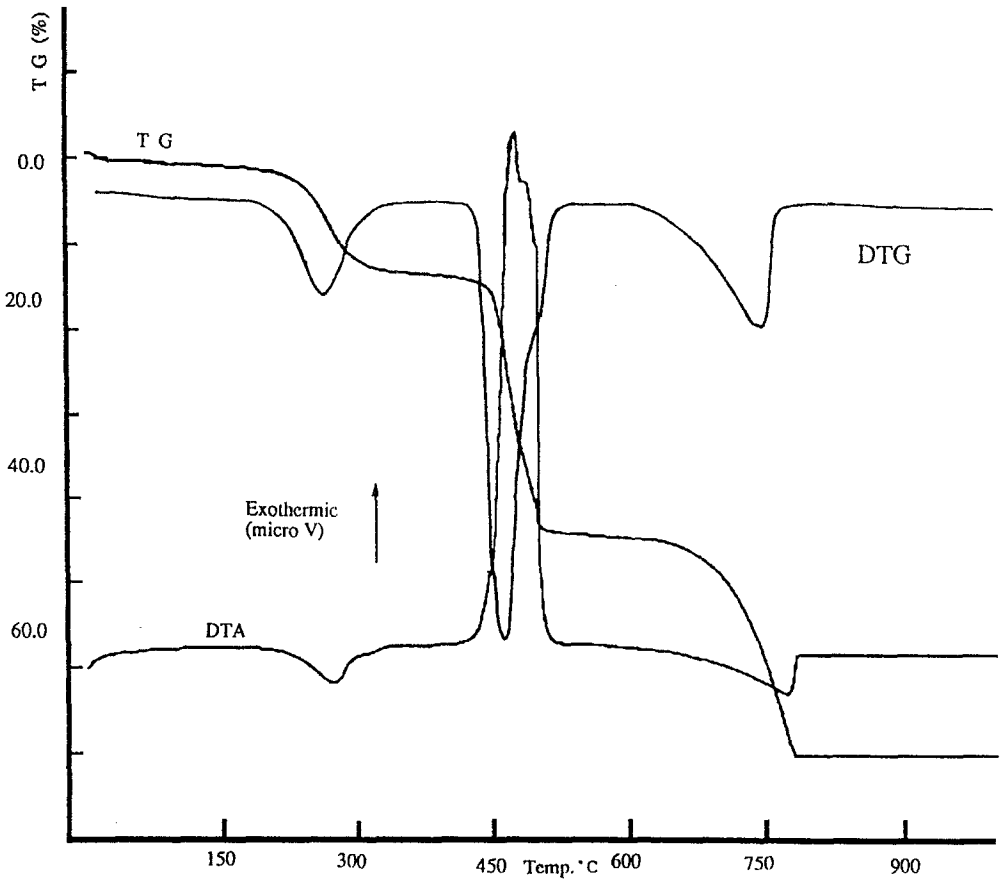

Fig. 1 TG/DTG and DTA curves for the decomposition of $Ca_3(C_6H_3O_6)_2 \cdot 3H_2O$ in flowing air atmosphere at 10°C min^{-1}

tile matter; the last with a minimum at 764°C, corresponds to the decomposition of calcium carbonate (calcite) to calcium oxide (lime), which was confirmed by XRD analysis to be the final product. The mass of the latter (33%) corresponds to the formation of 3 moles/mole of trihydrate (theoretical 32.6%).

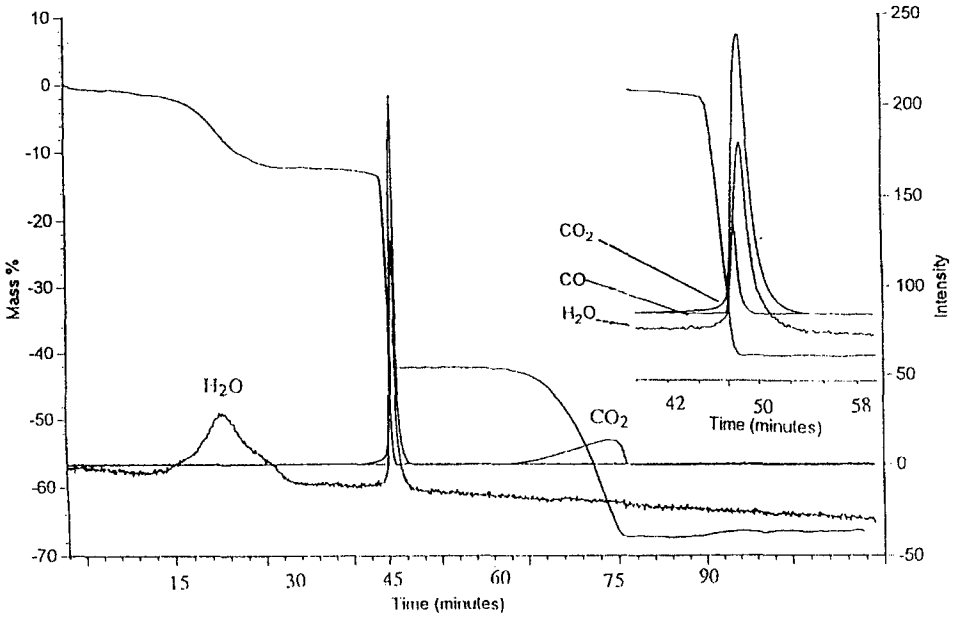

Fig. 2 EGA curves for the decomposition $Ca_3(C_6H_3O_6)_2 \cdot 3H_2O$ in an oxidising atmosphere at 10°C min^{-1}. The inset is an expansion of the EGA curves for the exothermic region

Figure 2 shows the mass loss and total evolved gases determined by EGA. The first and final mass losses were shown by IR analysis to be exclusively due to water and carbon dioxide evolution respectively. The mass loss from 428–507°C was found to coincide with the formation of carbon dioxide, water and carbon monoxide. Under the experimental conditions the presence of the latter is suggestive of incomplete oxidation of volatiles. These results support the interpretation of the TG and DTG curves, and to a certain extent the DTA curve. It is worthwhile to note that the decomposition of tricalcium aconitate parallels the decomposition of calcium oxalate monohydrate [14], dihydrate [15] and barium titanium citrate heptahydrate [16]: ie first dehydration occurs, then decomposition of the salt to the metal carbonate and finally decarboxylation of the carbonate to the oxide.

The TG/DTG and DTA curves for $Ca_2Mg(C_6H_3O_6)_2 \cdot 6H_2O$ are illustrated in Fig. 3. The TG curve shows three distinct mass losses at 77–290°C, 438–525°C and 661–756°C. The first corresponds to complete dehydration (20%) ie loss of six molecules of water and the remaining two stages (19 and 33%) are attributed to the decomposition of the anhydrous salt.

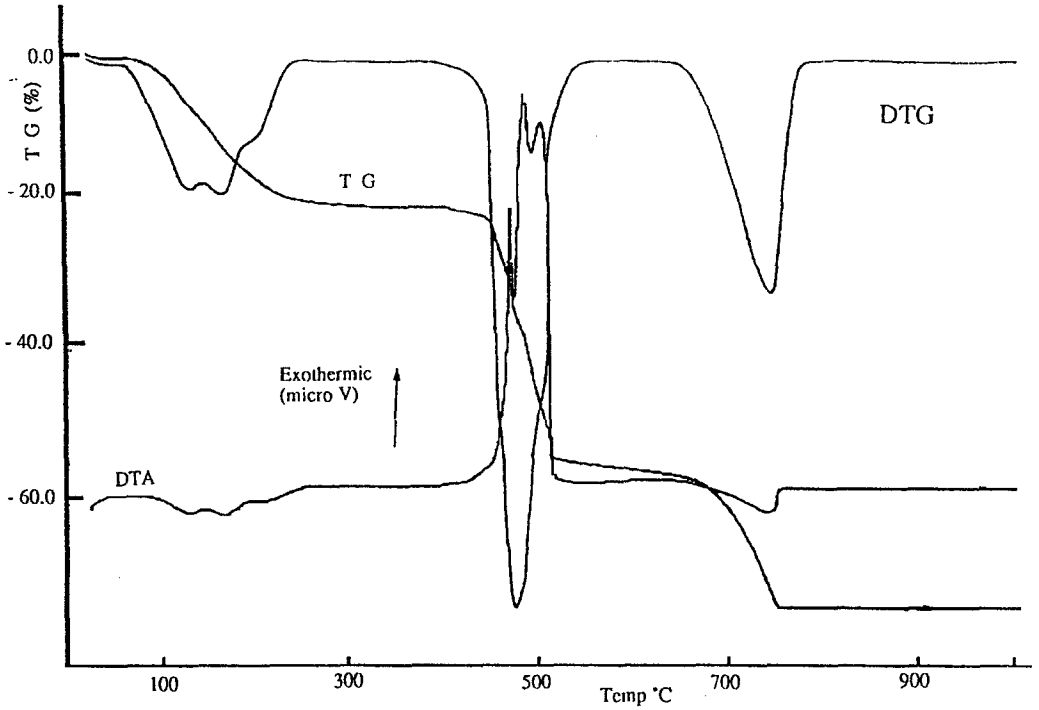

Fig. 3 TG/DTG and DTA curves for the decomposition of $Ca_2Mg(C_6H_3O_6)_2 \cdot 6H_2O$ in flowing air atmosphere at 10°C min^{-1}

The DTG and DTA curves of this salt show three overlapping reactions; the first occurring at 93–150°C corresponds to the loss of the first 2.0–2.5 water molecules, the second from 155–195°C represents the further loss of 2.0 water molecules and the last from 200–258°C the remaining 1.5–2.0 water molecules. There is another endothermic reaction from 661–756°C (peaking at 747°C) and an exothermic region with peak heights occurring at 479, 495 and 513°C, all associated with the decomposition events of anhydrous dicalcium magnesium aconitate. This exothermic region may also be influenced by the rearrangement of functional groups and change in molecular structure of this salt, in line with the suggestion of Mitchell and Knight [17] on the exothermic effects of cis-aconitic acid decomposition. The tricalcium aconitate is expected to behave similarly. The extra peaks observed in the exothermic peak region for the double salt can be attributed to the superposition of an endotherm due to the decarboxylation of the magnesium portion of the salt. XRD studies on a sample withdrawn at 515°C showed the presence of calcite and magnesium oxide (*d*-values at 2.11 Å and 1.49 Å). Finally the peak minimum at 747°C is again assigned to the decomposition of calcite to lime with the liberation of carbon dioxide. This event occurs 17°C below that observed with the tricalcium salt. This shift is due to the difference in crystal size between the two calcite minerals formed from their respective aconitate salts (as acertained from the XRD

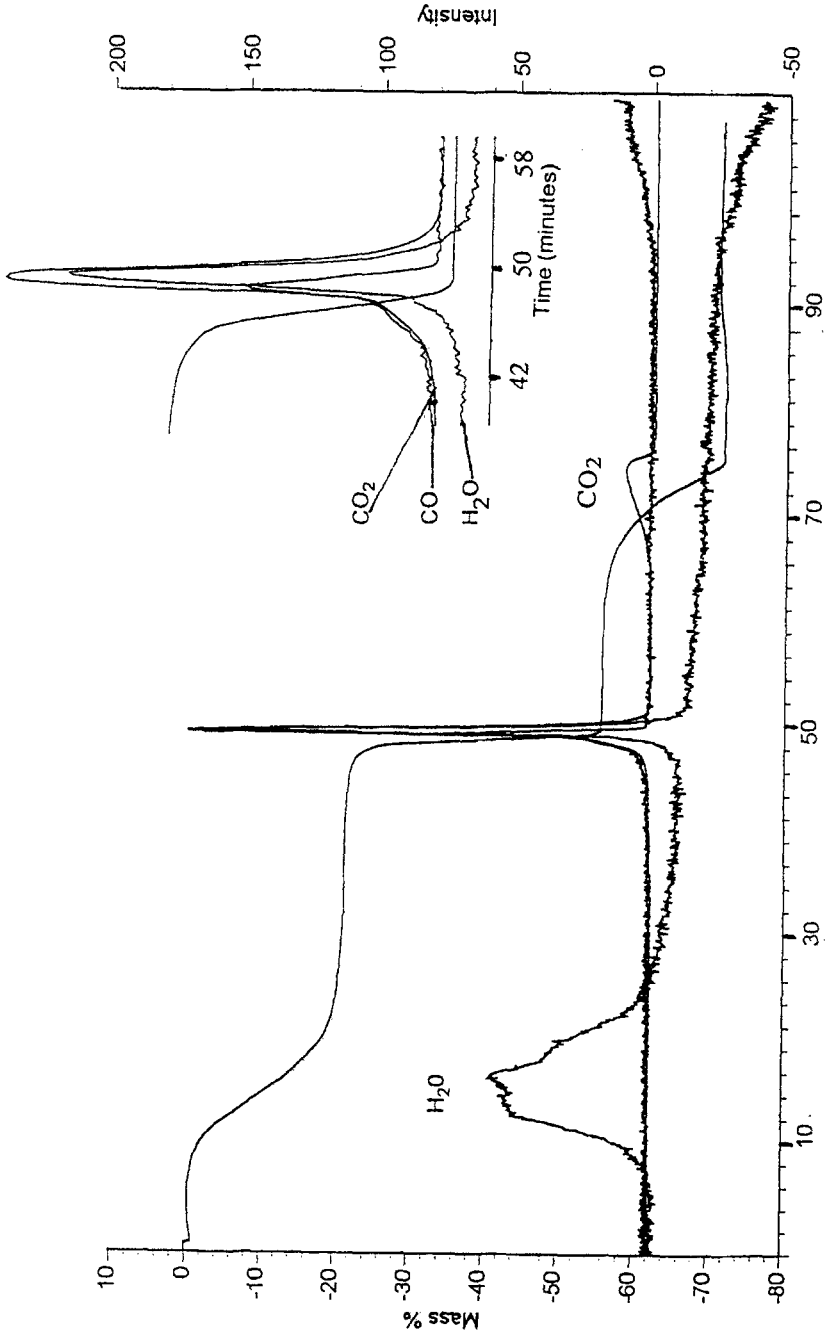

Fig. 4 EGA curves for the decomposition of $Ca_2Mg(C_6H_3O_6)_2.6H_2O$ in an oxidising atmosphere at 10°C min^{-1}. The inset is an expansion of the EGA curves for the exothermic region

spectra and SEM micrographs), and more definitively by the presence of magnesium oxide in the calcite matrix of the decomposed dicalcium magnesium aconitate. The final mass confirmed the formation of 2CaO and MgO/mole of double salt.

The EGA curves for $Ca_2Mg(C_6H_3O_6)_2 \cdot 6H_2O$ are shown in Fig. 4. It closely resembles that shown in Fig. 2 for $Ca_3(C_6H_3O_6)_2 \cdot 3H_2O$. It was noted however that in the exothermic region CO_2 was exclusively present at the commencement of decomposition/combustion process (428°C) in the case of the calcium salt (Fig. 2 inset), whereas both CO and CO_2 were present at a similar stage with the double salt (Fig. 4 inset). This observation may account for the difference in shape of the exotherm of the two salts in that temperature region. The ratio of CO to CO_2 over the complete exothermic region was also greater in the case of the double salt. This reduced oxidation of CO observed with the double salt is attributed to the influence of the endothermic formation of MgO as discussed above. However, it is possible that differences in crystal structure may also have an effect.

The first exothermic peak of the aconitates, which occurs at 477 and 479°C for the calcium and mixed calcium magnesium salts respectively, is very close to the single peak exotherm of calcium oxalate observed at 478°C [3, 4]. This peak in calcium oxalate has been attributed to the oxidation of carbon monoxide and the above peaks in the aconitates are of the same origin, as substantiated by the EGA results. The shoulder or extra peak at 495°C for the aconitates is associated with the oxidation of the hydrocarbon portion of these molecules to water and carbon dioxide. Boldyrev *et al.* [18] proposed a mechanism for the decomposition of the oxalates according to which the C–C bond breaks to yield CO_2^- radicals, and further work by Angelov and co-workers [19] have confirmed this. It would appear that this process precedes the complete fragmentation of the hydrocarbon portion of the aconitate. It might be expected that decomposition of the aconitates would involve the formation of itaconate and itaconic anhydride, as reported for aconitic acid [1] and barium titanium citrate hexahydrate ($BaTi(C_6H_6O_7)_3 \cdot 6H_2O$) [16]. However, there is no evidence for these intermediates in Figs 1 and 3 which resemble the DTA obtained with $Ba_2Ti(C_6H_5O_7)_2(C_6H_6O_7) \cdot 7H_2O$. The different behaviour is attributed to $BaTi(C_6H_6O_7)_3 \cdot 6H_2O$ having a partially ionised structure where as $Ba_2Ti(C_6H_5O_7)_2(C_6H_6O_7) \cdot 7H_2O$ and the aconitates have a higher degree of ionisation.

Crystal morphologies

Typical scanning electron micrographs for the hydrates and anhydrous salts are presented in Figs 5–8. Figure 5 shows well-developed twinned crystals of tricalcium aconitate trihydrate analogous in shape to swallow-tailed twins in calcium sulphate dihydrate. Stellate clusters consisting of more elongate crystals are intergrown with those possessing a flat platy morphology. Individual crystals in the stellate clusters are smaller with approximate dimension 10–15 μm in

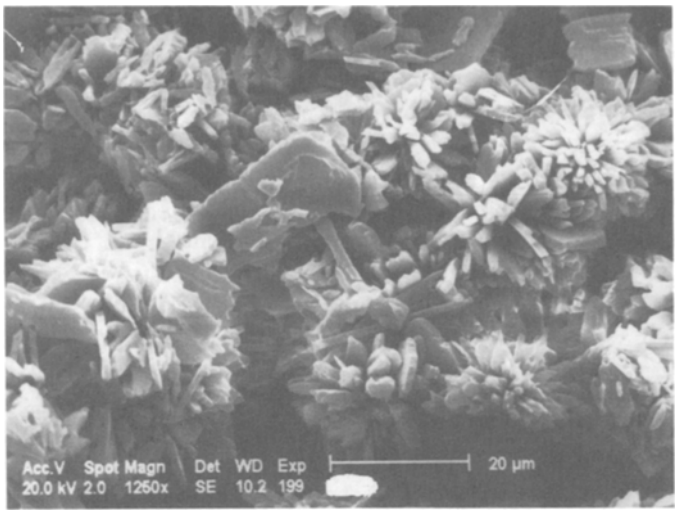

Fig. 5 Electron micrograph of tricalcium aconitate hydrate crystals

Fig. 6 Electron micrograph of anhydrous tricalcium aconitate crystals

length, 1.5–2.0 µm in width and 3–5 µm in thickness. The platy crystals are up to 25 µm long, 10–15 µm wide and 1–2 µm thick. The dehydrated crystals (Fig. 6) are very similar to those of the hydrate crystals, possibly with a greater abundance of swallow-tailed twins and less development of the larger platy crystals. Generally, the elongate crystals are smaller with a length less than 10 µm.

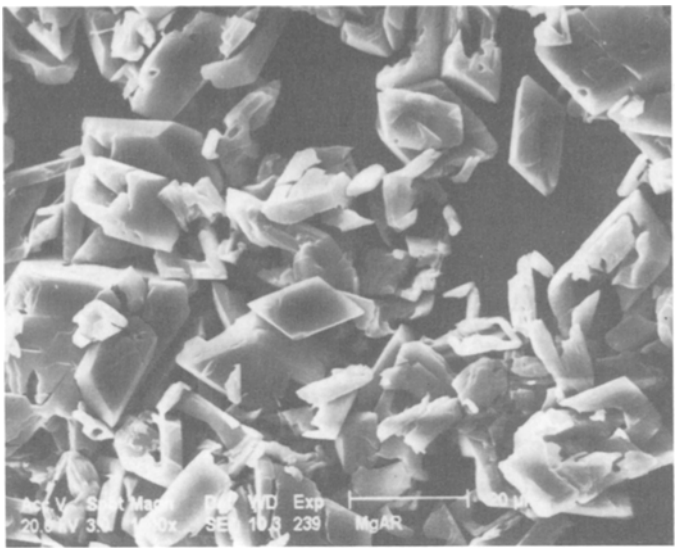

Fig. 7 Electron micrograph of dicalcium magnesium aconitate hydrate crystals

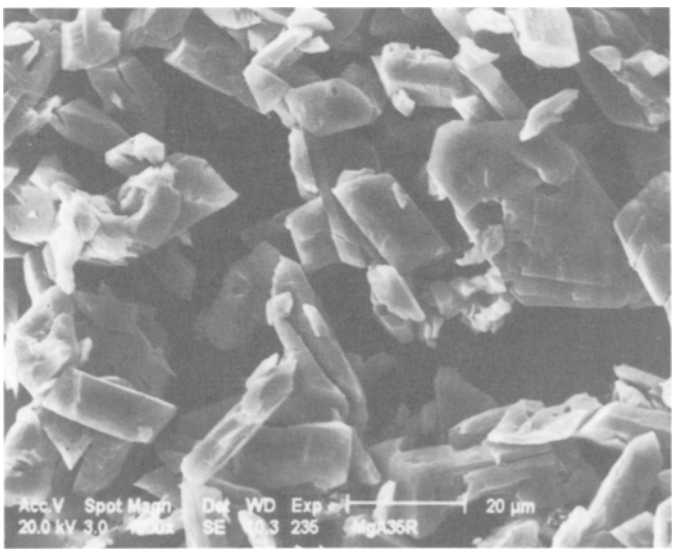

Fig. 8 Electron micrograph of anhydrous dicalcium magnesium aconitate crystals

Figures 7 and 8 give the micrographs of both the hydrate and anhydrous dicalcium magnesium aconitate. The hydrate crystals are predominantly in the 10–20 μm size range. The crystals are monoclinic with well-developed pinacoidal faces. In some crystals, monoclinic prisms and domatic forms are present.

The dehydrated form (Fig. 8) is also monoclinic but possibly with a smaller β-angle. Similar crystal shapes as the hydrates are also present but some are much more elongate and are of similar size. However, they frequently exhibit at least two well-developed cleavage directions at approximately 90°.

Kinetics of tricalcium aconitate trihydrate

Initial rate measurement at 221°C was calculated as 0.02/min using both the methods of Borchardt and Daniels [5] and Borchardt [13] respectively. The excellent agreement observed supports the application of the former method to the calculation of k_d and the energy of activation of the process. The DTA curve (Fig. 1) was analysed at different temperatures and k_d evaluated using Eq. (5) (Fig. 9). It is observed that k_d increased from 0.04/min at 238°C to greater than 0.86/min at 295°C.

Generally, the rates of formation of inorganic powder microcrystallites at any temperature can be expressed by the relation,

$$k_d = C_v \exp\frac{(-E_d)}{RT}\int[\alpha_d - (1 - \alpha_d)] \qquad (6)$$

C is a constant related to the number of water molecules per unit surface area of the powder particles: ν is the frequency factor and E_d is the energy of activa-

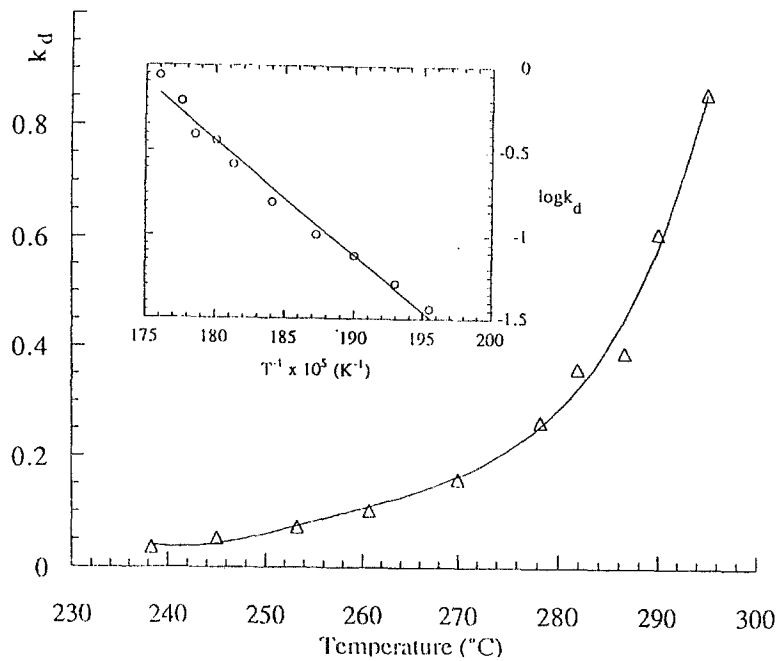

Fig. 9 The rate constant for tricalcium aconitate dehydration (k_d) *vs.* Temperature; Inset, $\log k_d$ *vs.* $1/T$

tion. When the rates are controlled by the interfacial reaction, ie as the active sites grow, the interface between the product and reactant increases, then

$$k_d = C_v \exp\frac{(-E_d)}{RT} \tag{7}$$

Figure 9 inset shows the Arrhenius plot of k_d data from which E_d was determined as 43±2 kJ mol^{-1} water. The value is comparable to nickel oxalate (68.5 kJ mol^{-1} water), manganese oxalate (50 kJ mol^{-1} water), calcium carbonate hexahydrate (25–30 kJ mol^{-1} water) and manganous formate hydrate 36.3±0.4 kJ mol^{-1} water), confirming the experimental observations that the hydrate water is attached to the metal cation.

* * *

The authors wish to thank the Sugar Research Development Corporation (SRDC) of Australia for financial support of the project.

References

1 P. Honig, Principles of Sugar Technology, Elsevier, Amsterdam 1964, Vol. 1, p. 142.
2 S. M. Paturau, By-products of the Can Sugar Industry, Elsevier, Amsterdam 1969, p. 238.
3 W. O. S. Doherty, O. L. Crees and E. Senogles, Cryst. Res. Technol., 28 (1993) 603.
4 W. O. Doherty, O. L. Crees and E. Senogles, Unpublished work.
5 H. J. Borchardt and F. Daniels, J. Am. Chem. Soc., 79 (1957) 41.
6 J. A. Ambler, J. Turner and G. L. Keenan, J. Am. Chem. Soc., 67 (1945) 1.
7 J. H. Sharp, Differential Thermal Analysis (R. C. Mackenzie, Ed.), Academic press, London 1972, Vol. 2, p. 47–77.
8 B. Locardi, Vetro Silicati, 7 (1963).
9 T. I. Barry, D. Cinton, L. M. Lay, R. A. Mercer and R. P. Miller, J. Material Sci., 4 (1969) 596.
10 D. Clinton, R. A. Mercer and R. P. Miller, J. Material Sci., 5 (1970) 171.
11 B. S. Girgis, Trans. But. Ceram. Soc., 71 (1972) 177.
12 W. O. S. Doherty, Ph. D. Thesis, London 1983.
13 H. J. Borchardt, J. Inorg. Nucl. Chem., 12 (1960) 252.
14 D. Dollimore and D. L. Griffiths, Thermal Analysis 1965, Macmillan 1965, p. 126.
15 W. O. S. Doherty, O. L. Crees and E. Senogles, Cryst. Res. Technol. 29 (1994) 517.
16 D. Hennings and W. Mayr, J. Solid State Chem., 26 (1978) 329.
17 B. D. Mitchell and A. H. Knight, J. Exp. Bot., 16 (1965) 1.
18 V. V. Boldyrev et al., Kinet. Catal., 11 (1970) 367.
19 S. Angelov and S. Stojanov, J. Phys. Chem. Solids, 67 (1985) 321.